A Direct Rotor Flux Controlled Induction Motor Drive for High Performance Applications

Sun-Soon Park and Gyu-Hyeong Cho

Department of Electrical Engineering
Korea Advanced Institute of Science and Technology
P.O. Box 150, Chongryang, Seoul, 131-650, Korea

Abstract

In this paper, a simple and high performance flux control scheme of induction motor is proposed. The flux in this drive is maintained constantly and controlled directly without any coupling to drive the induction motor like dc motor. The ripple current in this scheme is also bound using a double hysteresis loop(or delta modulation) to control the flux and the stator current simultaneously. It is verified through the simulation that the drive system using these methods operate well and have good dynamics in near zero-speed as well. Lastly, the simulation results are proved by experiment.

Introduction

In many application area such as servo and rolling mill, the drive system is required to have fast transient response and capability of operating near zero speed with full torque. For these purposes, cage type induction motor is attractive because of numerous merits, however, it is not easy to obtain the good dynamics since the induction machine is non-linear coupled system with complex multivariables.

The field oriented or vector control theories based on the synchronously rotating referenced d-q model of the machine can successfully solve the coupling problem[1]. In the direct method of the vector control, the information of the rotor flux is necessary to obtain the feedback signals whether it is computed or measured. In the indirect vector control method, the feedback signals (or command signals) are computed by means of the addition to the mechanical position vector of the rotor and the command slip angle vector derived from the torque component current. All of these methods require an amount of computation such as complex coordinate transformations and phase conversions. In addition it is not easy to find out the rotor flux vector accurately and instantaneously. In the direct vector control, not only the special machine is required because of sensing coil but the integration problem is included in near-zero speed, thus it is difficult for practical construction[2]-[4].

On the other hand, the rotor flux sensing method using the stator quantities is also very difficult in near-zero speed because it also has the integration problem and the stator resistance error effects seriously in the calculation of the rotor flux. Indirect method deeply depends on the machine parameter and the dynamic performance become poor when the parameters are changed[5].

In this paper, a direct rotor flux control method which be able to solve such problems is suggested. It is shown that the system operates well in near-zero speed with full torque. The merits of this scheme are verified through simulation results.

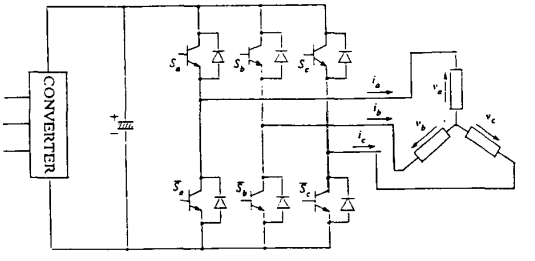

Fig. 1 A voltage source inverter for a 3-phase induction motor

Mathmatical Model of Induction Motor

A voltage source inverter for a 3-phase induction motor is shown in Fig. 1. The performance of the induction motor is analyzed with 3-phase variables in this paper. It is advantageous to use the 3-phase variables in the machine equations since the proposed control algorithm can be directly applied. A mathematical model of a voltage fed induction motor developed in actual machine variables is used to analize and implement the proposed scheme. The rotor equations in terms of the rotor flux linkages Ψ_r and stator current is refered to stationary reference frame are given by [6]

$$\frac{d\Psi_r}{dt} = a_r r_r \mathbf{i}_s + \mathbf{A}_r \Psi_r \tag{1}$$

where $a_r = L_m / L_r$

$$\mathbf{A}_r = \begin{bmatrix} -\frac{2}{3}\frac{r_r}{L_r} & \frac{1}{3}\frac{r_r}{L_r} - \frac{1}{3}\omega_r & \frac{1}{3}\frac{r_r}{L_r} + \frac{1}{3}\omega_r \\ \frac{1}{3}\frac{r_r}{L_r} + \frac{1}{3}\omega_r & -\frac{2}{3}\frac{r_r}{L_r} & \frac{1}{3}\frac{r_r}{L_r} - \frac{1}{3}\omega_r \\ \frac{1}{3}\frac{r_r}{L_r} - \frac{1}{3}\omega_r & \frac{1}{3}\frac{r_r}{L_r} + \frac{1}{3}\omega_r & -\frac{2}{3}\frac{r_r}{L_r} \end{bmatrix} \tag{2}$$

$$\Psi_r = \begin{bmatrix} \Psi_{ar} \\ \Psi_{br} \\ \Psi_{cr} \end{bmatrix} \qquad \mathbf{i}_s = \begin{bmatrix} i_{as} \\ i_{bs} \\ i_{cs} \end{bmatrix} \tag{3}$$

CH2721-9/89/0000-0279 $1.00 © 1989 IEEE

The phase voltages of the stator and the line voltages are given by (4) and (5).

$$\mathbf{v}_s = r_s \mathbf{i}_s + \sigma L_s \frac{d\mathbf{i}_s}{dt} + a_r \frac{d\Psi_r}{dt} \tag{4}$$

where $\mathbf{v}_s = \begin{bmatrix} v_{as} & v_{bs} & v_{cs} \end{bmatrix}^T$

$$v_{ab} = v_{as} - v_{bs};\quad v_{bc} = v_{bs} - v_{cs};\quad v_{ca} = v_{cs} - v_{as}. \tag{5}$$

The electromagnetic torque which is the rate of change of energy stored in the airgap can be evaluated by

$$T_e = \frac{1}{3}\frac{P}{2}\frac{L_m}{L_r}\left(\Psi_{ar}(i_{bs} - i_{cs}) + \Psi_{br}(i_{cs} - i_{as}) + \Psi_{cr}(i_{as} - i_{bs})\right) \tag{6}$$

Principle of Direct Rotor Flux Control Method

The basic idea of this method is to force the rotor flux to follow the appropriately given command flux at all states within a defined error bound. The command flux Ψ_r^* is given by (7) and the measured rotor flux $\hat{\Psi}_r$ can be calculated from (4) as (8). The error ϵ_ψ between the command and measured value is also shown in (9).

$$\dot{\Psi}_r^* = \omega_e \hat{\Psi}_r \mathrm{Re}\begin{pmatrix} e^{j\theta} \\ e^{j(\theta - 2\pi/3)} \\ e^{j(\theta + 2\pi/3)} \end{pmatrix} \tag{7-a}$$

$$\Psi_r^* = \hat{\Psi}_r \mathrm{Im}\begin{pmatrix} e^{j\theta} \\ e^{j(\theta - 2\pi/3)} \\ e^{j(\theta + 2\pi/3)} \end{pmatrix} \tag{7-b}$$

where $\omega_e = \omega_r + \omega_{sl}^*$, $\theta = \int(\omega_r + \omega_{sl}^*)dt$ and $\hat{\Psi}_r$ is the peak value of the command flux;

$$\dot{\hat{\Psi}}_r = \frac{L_r}{L_m}\left(\mathbf{v}_s - r_s \mathbf{i}_s - \sigma L_s \frac{d\mathbf{i}_s}{dt}\right) \tag{8-a}$$

$$\tilde{\Psi}_r = \frac{L_r}{L_m}\int(\mathbf{v}_s - r_s \mathbf{i}_s - \sigma L_s \dot{\mathbf{i}}_s)\, dt \tag{8-b}$$

$$\epsilon_\psi = \hat{\Psi}_r - \tilde{\Psi}_r \tag{9-a}$$

or

$$\epsilon_\psi = \int(\dot{\Psi}_r^* - \dot{\hat{\Psi}}_r)\, dt \quad . \tag{9-b}$$

On the other hand, (10) is obtained from (1)-(2), which show that the rotor flux can be controlled by the stator voltages:

$$\frac{d^2\Psi_r}{dt^2} = -\frac{r_s + a_r^2 r_r}{\sigma L_s}\mathbf{I} + \mathbf{A}_r \frac{d\Psi_r}{dt} + \frac{r_s}{\sigma L_s}\mathbf{A}_r \Psi_r + \frac{r_r}{\sigma L_s}\mathbf{v}_s \tag{10}$$

The block diagram to regulate the actual flux (and measured flux) with the command flux is shown in Fig 2. In this block diagram, the hysteresis has the characteristics as

$$\begin{aligned} -\Delta\Psi_r < \epsilon_\psi < \Delta\Psi_r \quad & \mathbf{S} \text{ state is not changed} \\ \epsilon_\psi > \Delta\Psi_r \quad & S^+ \rightarrow S^- \quad \epsilon_\psi \rightarrow 0 \\ \epsilon_\psi < -\Delta\Psi_r \quad & S^- \rightarrow S^+ \quad \epsilon_\psi \rightarrow 0 \end{aligned}$$

where $\mathbf{S} = \begin{bmatrix} S_A & S_B & S_C \end{bmatrix}^T$.

This illustration shows that the actual flux is controlled by the hysteresis control algorithm and the error between the command and actual flux is bound within a small specified value. Thus the actual flux has some ripple, however, and if this error bound is restricted to a very small value so that it is negligible, the electromagnetic torque can be written as

$$T_e = \frac{3}{2}\frac{P}{2}\frac{\hat{\Psi}_r^2}{r_r}\omega_{sl} \quad . \tag{11}$$

This equation show that the torque is directly proportional to the slip frequency ω_{sl} without any delay time because it is not only true in steady state but in transient as long as when the magnitude of the flux (or command flux) maintains constant value. In other words, it means that the electromagnetic torque is instantaneously generated and linearly controlled by the slip frequency ω_{sl} .

If it is assumed that the rotor flux are exactly controlled with the command value, the stator currents in steady state are regulated with

$$\mathbf{i}_s = \frac{\omega_{sl}}{a_r r_r}\hat{\Psi}_r \mathrm{Re}\begin{pmatrix} e^{j\omega_e t} \\ e^{j(\omega_e t - 2\pi/3)} \\ e^{j(\omega_e t + 2\pi/3)} \end{pmatrix} + \frac{\hat{\Psi}_r}{L_m}\mathrm{Im}\begin{pmatrix} ej(\omega_e t) \\ e^{j(\omega_e t - 2\pi/3)} \\ e^{j(\omega_e t + 2\pi/3)} \end{pmatrix} \tag{12}$$

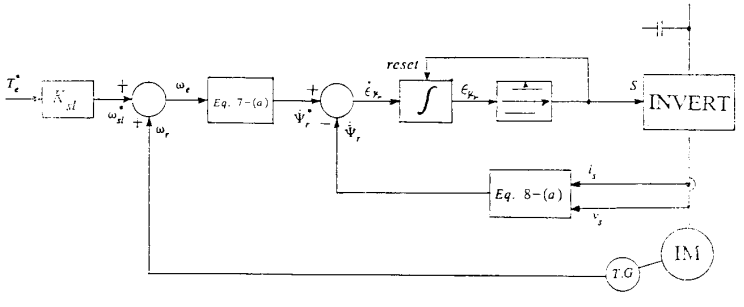

Fig. 2 Direct rotor flux control scheme

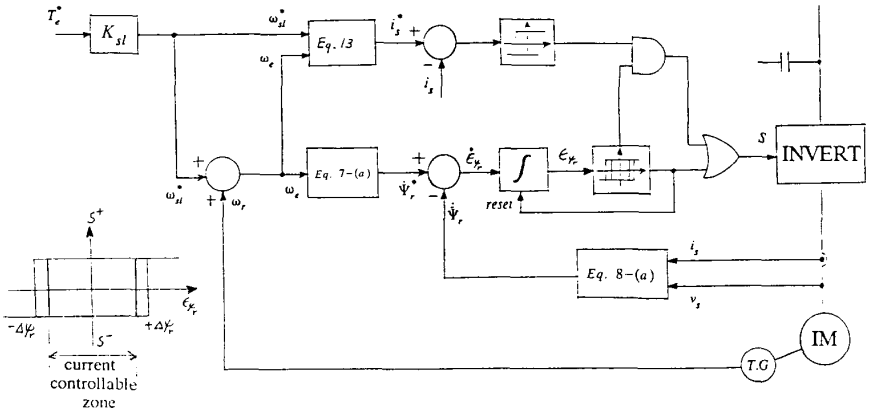

Fig. 3 Direct rotor flux control scheme including double hysteresis method

The measured error of the rotor flux in this system is reseted instead of being accumulated at when the hysteresis state is changed so that the error exists in a given boundary. Besides, the measured flux error can be reduced due to the operation of the feedback because the flux loop is closed. This action is thought to be one of the merits when compared with the conventional vector control method and the effect is shown well through the simulation results.

Double Hysteresis Control Method

In the steady state, the previous section showed that the stator currents are controlled by the slip frequency. However the ripple current is not bounded to a value, rather it is determined by the input voltage of the inverter, the switching frequency and the leakage inductance of the induction motor, etc. Examining of (10), we know that the rotor flux equation is expressed by the double integral form as for the stator voltage, then the rotor flux response which is controlled by the stator voltage is delayed. Also the hysteresis interval for the rotor flux control must not be less than some value in practical implementation. Therefore, the ripple current is increased because the inverter switching frequency is limited to some value. This problem is a disadvantage of this method, however, it can be easily solved by double hysteresis control described below.

A double hysteresis control method is a simultaneous control of the rotor flux and the stator current by means of controlling the stator voltage. Fig. 3 shows the operation of this method. In this block diagram, another hysteresis zone to control the stator current is established together with the zone for controlling the rotor flux. If the flux error between the command and measured values exist in the range of the current controllable zone, the hysteresis action for stator current control operates. In this case, the stator current command cab be written by

$$\mathbf{i}_s^* = I_T^* \mathrm{Re}\begin{pmatrix} e^{j\omega_e t} \\ e^{j(\omega_e t - 2\pi/3)} \\ e^{j(\omega_e t + 2\pi/3)} \end{pmatrix} + \frac{\hat{\Psi}_r}{L_m} \mathrm{Im}\begin{pmatrix} e^{j\omega_e t} \\ e^{j(\omega_e t - 2\pi/3)} \\ e^{j(\omega_e t + 2\pi/3)} \end{pmatrix} \qquad (13)$$

where

$$\omega_e = \omega_r + \omega_{sl}^* \qquad (14)$$

$$\omega_{sl}^* = \frac{a_r r_r^* I_T^*}{\hat{\Psi}_r} \qquad (15)$$

Besides the upper illustrations, the current ripple is greatly reduced without sacrificing the accurate rotor flux control and without dynamic loss, if the double hysteresis is used.

Consideration for Efficient Control

In the previous sections, it was been shown that the rotor flux can be controlled accurately and quickly using the direct rotor flux control method. Torque and speed responses can also be made fast even when the magnitude of the rotor flux is adjusted.

From this result, it is possible to apply this method to control the induction motor efficiently. Therefore this section deals with the efficient operation of the induction motor which is accomplished by the rotor flux magnitude control without dynamic loss.

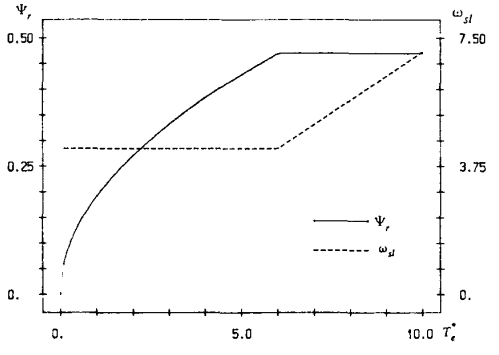

Fig. 4 Flux level and slip frequency for obtaing maximum efficiency

The rotor flux level should be maintained to its maximum value for heavy load, however, the magnitude can be controlled at light load, resulting in low the iron losses. For this reason, the copper loss which is the dominant losses of the induction motor in the controllable region of the rotor flux can be obtained from (12) as

$$P_{loss} = 3I_s^2 r_s + 3I_r^2 r_r \tag{16}$$

or

$$P_{loss} = 3((\omega_{sl}/a_r r_r)^2 + 1/L_m^2)\, r_s \hat{\Psi}_r^2 + 3\omega_{sl}^2 \hat{\Psi}^2 / r_r \quad . \tag{17}$$

Substituting (11) to (16), the loss equation is rearranged as

$$P_{loss} = 3\frac{r_s}{L_m^2}\hat{\Psi}_r^2 + \frac{16}{3P^2}(r_s/a_r^2 + r_r)T_e^2\hat{\Psi}_r^{-2} \quad . \tag{18}$$

From (18), if the output torque is constant, the loss is a function of the rotor flux only. Then the minimum value of the loss and the flux magnitude can be determined by solving $\hat{\Psi}_r$ setting $dP_{loss}/d\hat{\Psi}_r = 0$.
The solution becomes

$$\hat{\Psi}_{r\eta} = \left(\frac{16}{9P^2}L_r^2\frac{r_s + a_r^2 r_r}{r_s}T_e^2\right)^{1/4} \tag{19}$$

$$P_{loss\ \min} = \frac{8}{P}\frac{L_r}{L_m^2}\sqrt{r_s(r_s + a_r^2 r_r)}\, T_e \quad . \tag{20}$$

When the motor operates at its the maximum efficiency, the slip frequency is determined by

$$\omega_{sl\eta} = \sqrt{\frac{r_s}{r_s + a_r^2 r_r}}\frac{1}{T_r} \quad . \tag{21}$$

From (20) and (21), we know that the loss in this efficient control is proportional to the output torque and the slip frequency is determined by the motor parameters only. The flux level and slip frequency which gives the maximum efficiency as a function of the output torque are shown in Fig. 4 where the flux level is limited to 0.47 for non-saturation.

The addition of the flux magnitude control loop for efficient control can be hard on the stability. But this problem can be easily solved because the fast response of the flux magnitude control only require when incresing of the flux magnitude. In other words, the flux magnitude for obtaing good dynamics directly propertional to the torque command when the torque command is increased, but very slowly reduce when the torque command is decrease. This action can be acomplished by a peak detector.

Simulation Results

Simulations are performed using 5 Hp induction motor given in Table 1 and 2 . This induction motor is modeled under stationary reference frame in the abc-axis. The drive system is constructed using voltage source type PWM inverter. Fig. 5 shows the simulation results during an acceleration interval from 1000 *rpm* to 1200 *rpm* when the double hysteresis control method is not applied (a) and applied (b) in respectively. Both Figures show that the rotor flux accurately follow the command value throughout the period and the output torque is instantaneously controlled with quick speed response.

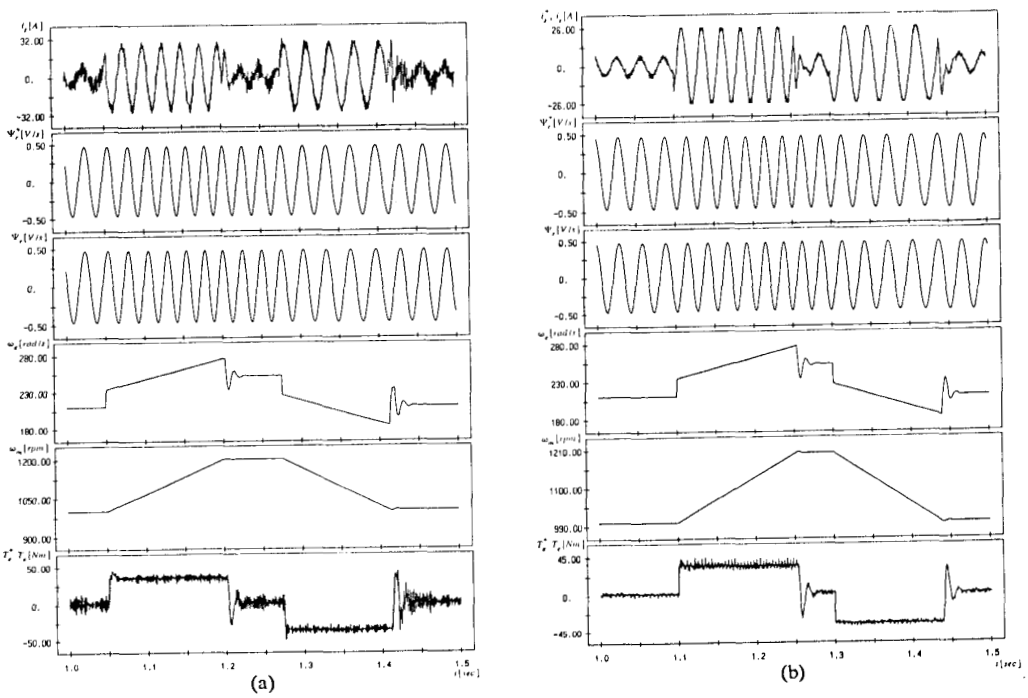

Fig. 5 Simulation results during acceleration and deceleration interval between 1000 *rpm* and 1200 *rpm* when the double hysteresis control is not applied (a) and applied (b) .

The only differences (a) and (b) are that the ripple current and torque with the double hysteresis control method are much smaller than those with the single hysteresis method.

Fig. 6 shows the phenomenon during abrupt torque command change in between 5 *Nm* and 15 *Nm* for both double (b) and single (a) hysteresis control cases, respectively. In this case, it is shown that the flux magnitude is not changed and the torque response is also quick. Both cases are almost the same except the magnitude of the current and torque ripples. As described in section III, since the hysteresis interval for the rotor flux control must not be less than some value in practical implementation, the maximum switching frequency is limited to 1 *K Hz* when the single hysteresis control method is used and 5 *K Hz* when the double is used. In this case, the hysteresis interval $\Delta\Psi_r$ are set to be the same value of 0.01 .

The capability for the maximum efficiency control without dynamic loss is illustrated in the previous section. The methods

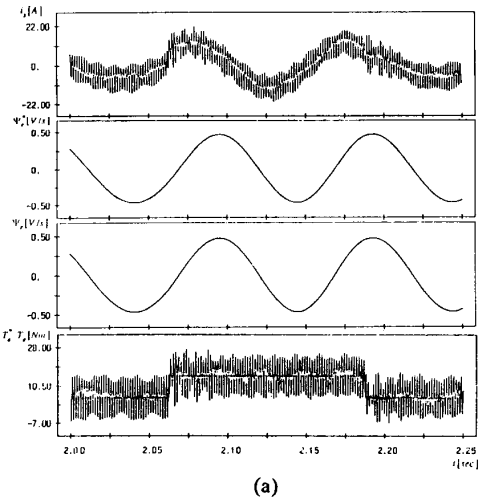

(a)

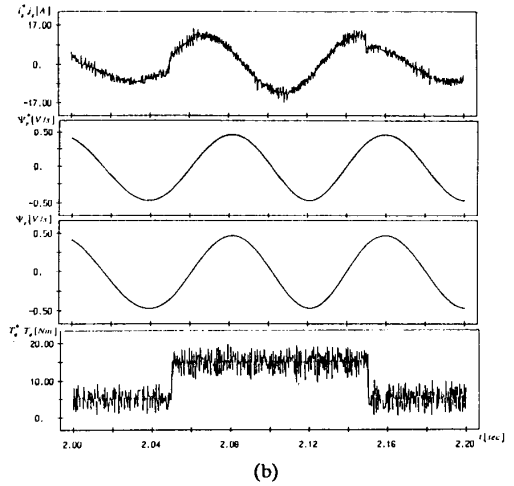

(b)

Fig. 6 Torque response when the torque command is abruptly changed for both (a) single (b) double hysteresis control case.

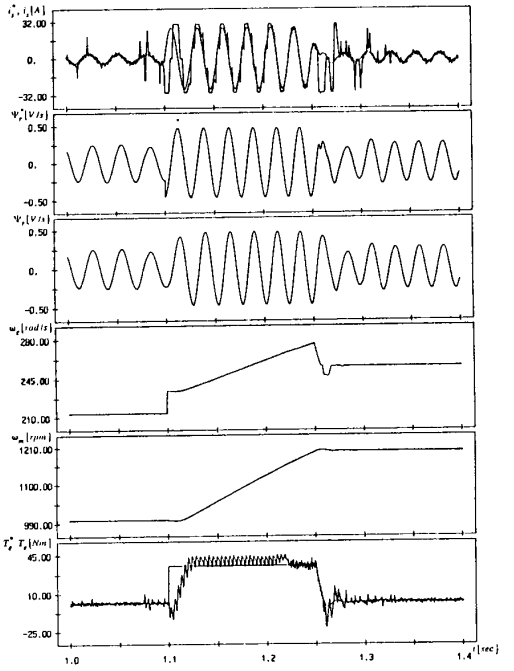

(a)

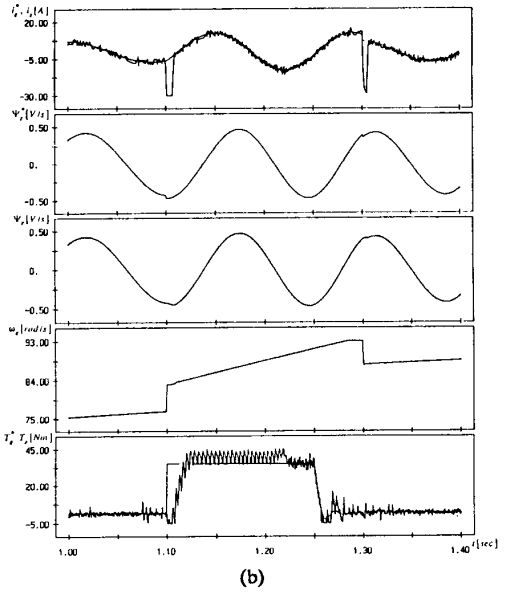

(b)

Fig. 7 (a) Speed and (b) torque response when the flux level is controlled as torque command.

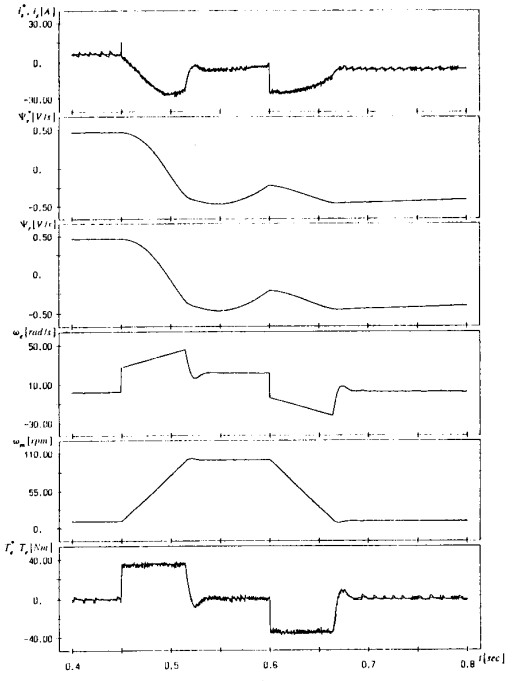

(a)

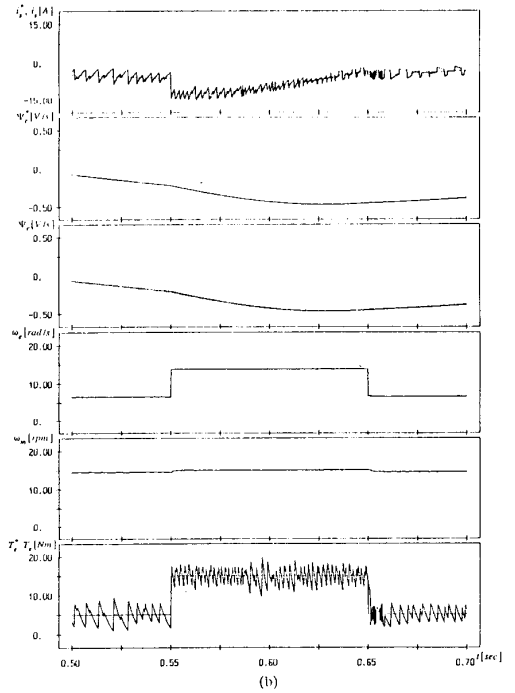

(b)

Fig. 8 (a) Speed response when the speed command is abruptly changed from 10 to 100 *rpm* and 100 to 10 *rpm*, (b) Torque response in low speed operation (15 *rpm*).

Table 1

Name – plate motor data
5 HP
Y – connected
$V_{rated} = 220V_{rated}$
$I_{rated} = 14A$
$N_{rated} = 1735rpm$
Four – pole
$J = 0.12 Kg \cdot m^2$
$B = 0.0082 Kg \cdot m^2/sec$

Table 2

Motor parameter
$r_s = 0.50\,\Omega$
$r_r = 0.47\,\Omega$
$L_s = 77.3\,mH$
$L_r = 78.9\,mH$
$L_m = 76\,mH$

are to control the rotor flux and the slip frequency as (19) and (21) sequencially. Fig. 7 (a) and (b) show the speed and torque responses when the flux is controlled by the torque command. These results illustrate that the flux is almost instantaneously controlled and the output torque is generated with small delay.

Fig. 8-(a) shows a step response of rotating speed change from 10 to 100 *rpm* for double hysteresis case. This result shows that the dynamic performance is very good, even around the zero speed. Fig. 8-(b) shows that a torque response in 10 *rpm* operation is also good when the torque command is abruptly changed. Fig. 9 show the dynamic performance when the stator resistance is incresd to 20 % and so the measured value of the stator resistance is incorrect. From this result, we know that the system is robust in stator resistance variation.

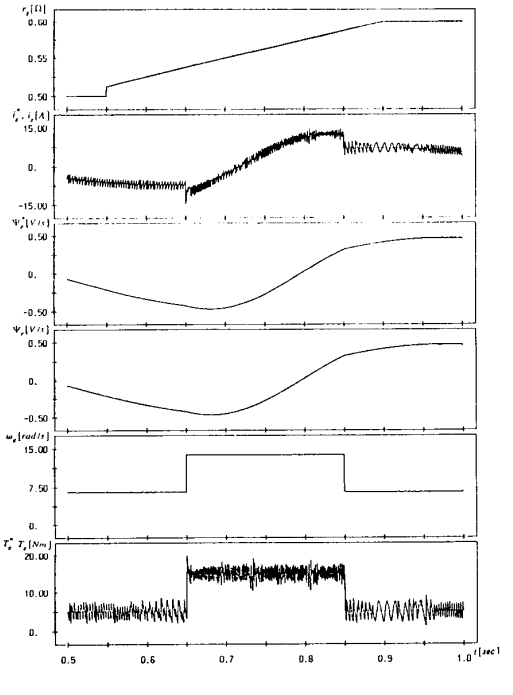

Fig. 9 Dynamic characteristics in low speed operation when stator resistance is increased.

Experimental Results

Experiments were carried out using 5 hp induction motor coupled to a dc-generator which adds to the shaft inertia. The parameters of IM were the same as those used for the simulation. The experiments also were performed with the double hysteresis control method using voltage source type PWM inverter.

Fig. 10 show the oscillograms of the stator voltage and the airgap voltage of A-phase when the motor run at 1000 *rpm* with half load. The ripple in the airgap voltage is due to slightly detuning of the stator parameters. Although the stator parameters are slightly detuned, it is almost not sacrificing of the system performance.

Fig. 11 show the experimental results during an acceleration and deceleration interval in between 1000 *rpm* and 1200 *rpm*. Both the stator current and speed are in good agreement with simulation result in Fig. 5-(b). Fig. 12 show the speed reversal characteristic when the speed command is abruptly changed from -300 *rpm* to 300 *rpm*. The phase inversion of the stator current is also shown in this Figure. Fig. 13 show the closed loop response for the abruptly load change in between 5 *Nm* and 15 *Nm* when the motor runs at 300 *rpm*. The settling time, refered to speed, is in the range of 100 t0 150 *ms*.

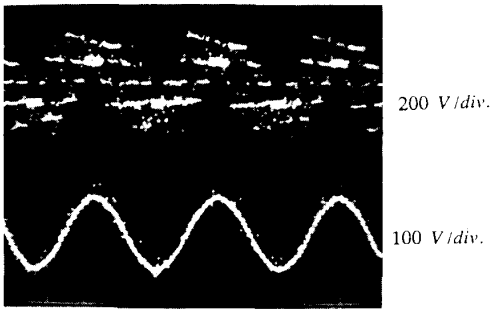

Fig. 10 Oscillograms of the stator voltage and the airgap voltage of A-phase when the motor runs at 1000 *rpm*.

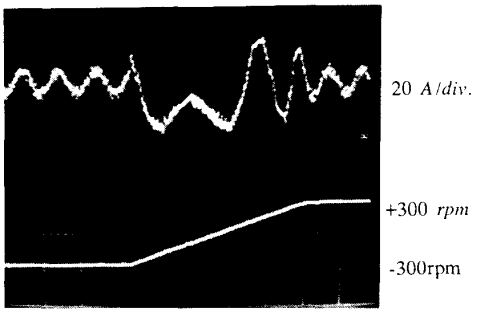

Fig. 12 Speed reversal characteristics when the speed command is abruptly changed from -300 to +300 *rpm* : 100 *ms/div.*

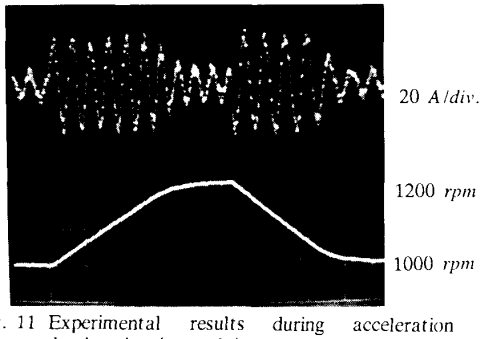

Fig. 11 Experimental results during acceleration and deceleration interval in between 1000 and 1200 *rpm* : 50 *ms/div.*

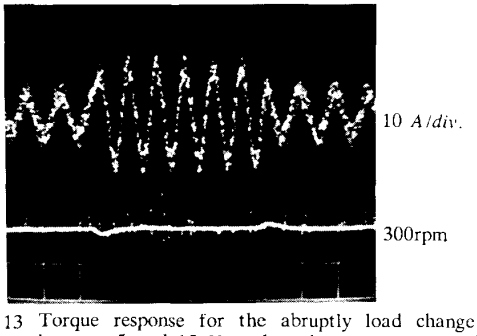

Fig. 13 Torque response for the abruptly load change in between 5 and 15 *Nm* when the motor runs at 300 *rpm* : 100 *ms/div.*

Conclusion

A direct rotor flux control method to drives the induction motor with high performance is proposed and analytically described in this paper. This method has many advantages such as constant rotor flux even during transient interval, simple construction and robustness against parameter variations. Also, the system has good dynamics and operates well in near-zero speed. Since the rotor flux can be instantly controlled without any coupling, the induction motor can be drived with reduced field condition at light load.

One demerit of this system is that the ripple current magnitude somewhat higher than that of the CRPWM type if single hysteresis control is used. However, the ripple magnitude is also successfully reduced by employing double hysteresis control method.

REFERENCES

[1] F. Blaschke, "The principle of field orientation as applied to the new transvector closed-loop control system for rotating field machines," *Siemens Rev., vol.34. pp.217-220,* 1972.

[2] M. Akamatsu, "High Performance IM Drive by Coordinate Control Using a controlled Current Inverter," *IEEE Trans. Ind. Appl. vol.IA-18, NO.4, pp.382-392,* July/August 1982.

[3] R. Gabriel and W. Leonhard, "Microprocessor Control of Induction Motor,"
in Conf. Rec., IAS 1982 Annu. Meeting pp. 385-396

[4] K. B. Nordin, D. W. Novotny and D. S. Zinger, "The influence of Moter Parameter Deviations in Feedforward Field Orientation Drive Systems," *in Conf. Rec. IAS 1984 Annu. Meeting pp. 525-531*

[5] R. Krishnan and F. C. Doran, "Study of Parameter Sensitivity in High Performance Inverter-Fed Induction Moter Drive System,"
IEEE Trans. Ind. Appl., vol.IA-23 No4, July/August 1987

[6] S. Yuvarajan, Bellakonda Ramaswami and V. Subrahmanyam, "Analysis of a Current-Controlled Inverter-fed Induction Moter Drive Using Digital Simulation," *IEEE Trans. Ind. Elec., vol.IECI-27 NO.2 May 1980*